Dipole-Supported Electronic Resonances Mediate Electron-Induced Amide Bond Cleavage

Zhou Li,[1,2,*] Michal Ryszka,[1,*] M. Michele Dawley,[1] Ian Carmichael,[1] Ksenia B. Bravaya,[3,†] and Sylwia Ptasińska[1,2,‡]
[1]*Radiation Laboratory, University of Notre Dame, Notre Dame, Indiana 46556, USA*
[2]*Department of Physics, University of Notre Dame, Notre Dame, Indiana 46556, USA*
[3]*Department of Chemistry, Boston University, Boston, Massachusetts 02215, USA*

(Received 15 July 2018; revised manuscript received 11 October 2018; published 21 February 2019)

Dissociative electron attachment (DEA) plays a key role in radiation damage of biomolecules under high-energy radiation conditions. The initial step in DEA is often rationalized in terms of resonant electron capture into one of the metastable valence states of a molecule followed by its fragmentation. Our combined theoretical and experimental investigations indicate that the manifold of states responsible for electron capture in the DEA process can be dominated by core-excited (shake-up) dipole-supported resonances. Specifically, we present the results of experimental and computational studies of the gas-phase DEA to three prototypical peptide molecules, formamide, *N*-methylformamide (NMF), and *N*,*N*-dimethylformamide (DMF). In contrast to the case of electron capture by positively charged peptides in which amide bond rupture is rare compared to N─C_α bond cleavage, fragmentation of the amide bond was observed in each of these three molecules. The ion yield curves for ions resulting from this amide bond cleavage, such as NH_2^- for formamide, $NHCH_3^-$ for NMF, and $N(CH_3)_2^-$ for DMF, showed a double-peak structure in the region between 5 and 8 eV. The peaks are assigned to Feshbach resonances including core-excited dipole-supported resonances populated upon electron attachment based on high-level electronic structure calculations. Moreover, the lower energy peak is attributed to formation of the core-excited resonance that correlates with the triplet state of the neutral molecule. The latter process highlights the role of optically spin-forbidden transitions promoted by electron impact in the DEA process.

DOI: 10.1103/PhysRevLett.122.073002

Low-energy electrons (LEE), formed in secondary processes that accompany high-energy light-matter interactions, are the key players in radiation damage of biomolecules, including DNA [1] and proteins [2]. These electrons can be temporarily trapped to form transient negative ion (TNI) species, which further undergo electronic and structural transformation leading to fragmentation [Fig. 1(a)], a process called dissociative electron attachment (DEA). LEE-induced damage to DNA was first experimentally demonstrated by Sanche and co-workers who showed that LEE irradiation resulted in single- and double-strand breaks in DNA [3]. Since then, many experimental and theoretical works [1,4–8] have been devoted to the LEE-induced fragmentation of biomolecules to obtain a comprehensive picture of the damage mechanism. It has been shown that shape [Fig. 1(b)] resonances are mostly responsible for single-strand breaks in the low-energy range (0–3 eV) [9–11], whereas shake-up resonances cause both single- and double-strand breaks for higher energy electrons [1,12]. The mechanisms of peptide interaction with slow electrons are even more complex due to both the structural diversity and the heterogeneous charge distribution.

The peptide bond is the basic linkage in proteins. Thus, it is one of the most widely existing structural motifs in nature. Peptides also play an important role in a host of biological activities in organic systems. In clinical studies, several inhibitory peptides have been confirmed to be effective in the treatment of cancers and other diseases [13,14]. Because secondary electrons are the most abundant species among all of the daughter species produced by

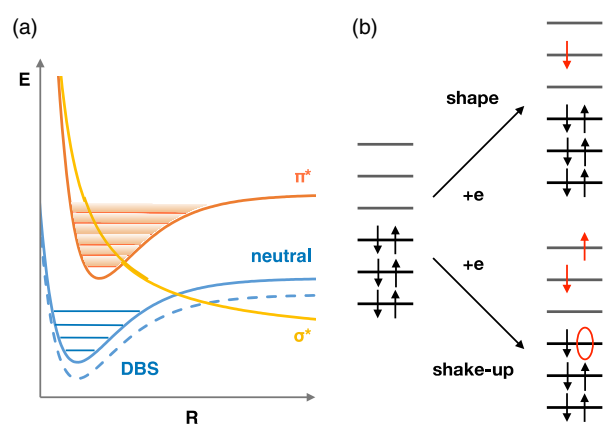

FIG. 1. Electronic states relevant for DEA processes. (a) Schematic potential energy curves of an initial neutral, dipole-bound state (DBS) and anionic π^* and σ^* states populated upon electron attachment. (b) Electronic configuration of shape and shake-up (core-excited) resonances.

 © 2019 American Physical Society

radiation in cells [15] a study of the impact of LEEs on peptides is critical to discover the potential radiation damage pathways involving proteins. This knowledge will be essential for improving radiotherapy, which is currently the most widely adopted treatment for cancer. Additionally, because of the bond-specific fragmentation pattern that is manifested by DEA [4,16–18], this mechanism is very promising for engineering new techniques for compound analysis. One example is the utilization of electron capture dissociation in peptide and protein sequencing using tandem mass spectrometry [19–21]. For this purpose, positively charged gas-phase peptides are irradiated with low-energy electrons. The identities and abundances of the electron attachment-induced fragment ions are then monitored by a mass spectrometer. Because this method selectively cleaves disulfide and N—C_α bonds, characterization of the peptides can be achieved by analyzing the mass spectra. Although this technique has been successfully applied to many different types of polypeptides, the detailed mechanisms of electron attachment-induced dissociation and the nature of the TNIs produced in peptides are still poorly understood.

Whereas the main dissociation channels for charged peptides and peptide radicals are associated with N—C_α and S—S bond cleavage, the products formed upon dissociation along the peptide bond have also been observed [21]. Here, we focus on the mechanism of the electron-capture-induced cleavage of a peptide bond by considering several prototypical neutral systems. Depending on the energetics of electron attachment, reactive electron scattering on a neutral molecule can lead to the formation of either bound states of the anion or transient negative ion states, which are states that are metastable with respect to electron ejection. Special care should be taken when theoretically describing these metastable electronic states, i.e., resonances. Electron capture can be rationalized in terms of the population of unoccupied π^* or σ^* virtual orbitals, i.e., the formation of shape valence resonances or the formation of core-excited resonances when two of the initially unoccupied orbitals become populated [Fig. 1(b)]. Dipole bound states (DBS) that are often coupled to valence metastable states have previously been discussed as the key players in low-energy DEA for molecules with large enough dipole moments [22–26]. While DEA processes in prototypical biomolecules have been extensively studied by both experiments and theory, a complete mechanistic picture remains elusive.

Here, we present results from a comprehensive computational and experimental investigation on the DEA to gas-phase formamide [Fig. 2(a)], the smallest prototype of a peptide, and its methylated derivatives, *N*-methylformamide [NMF, Fig. 2(b)], and *N*,*N*-dimethyl-formamide [DMF, Fig. 2(c)]. Experimentally, the ion yield curves for the anions as a function of the incoming electron's energy were measured [27]. High-level electronic structure calculations were exploited to interpret the experimental

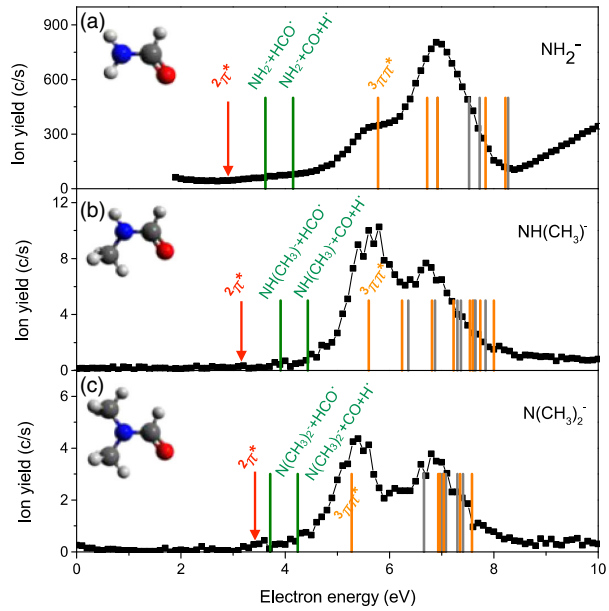

FIG. 2. Dissociative electron attachment ion yield curves for formamide (a), NMF (b), and DMF (c). Computed position of π^* resonances (red arrow), thermodynamic thresholds (green), energies of singlet (gray), and triplet (orange) excited states of the neutrals with large enough dipole moment to bind an electron are shown.

results, i.e., to identify the most efficient electron capture channels responsible for formation of the TNIs in the experimentally observed energy range.

Electron attachment to gas phase formamide, NMF, and DMF can cause the parent molecules to fragment into several pathways [57]. Here, we focus on amide bond cleavage. A detailed discussion of the ion yield curves for all anionic fragments is beyond the scope of the present work; however, our data agree well with the results of previously reported measurements for formamide and NMF [33,57]. It is well known that large polypeptides can break down into small fragments via bond cleavage in the backbone via the capturing of low-energy electrons [19,58]. In the case of low-energy electrons attaching to positively charged peptides, N—C_α bond rupture is reported to be the dominant pathway for breaking the peptide backbone [20]. In contrast, N—C_α bond cleavage, i.e., N-CH_3 in NMF and DMF, leading to anion formation was not observed in DEA to neutral small peptide model molecules. Note that neutral fragments are challenging to detect [59], and any channels leading exclusively to neutral fragments (i.e., no anion fragment) are not considered here. However, the amide bond, (C = O)-N, was found to be damaged in all the molecules investigated here, and it occurs in a similar energy region.

The simple amide bond cleavage breaks the molecules into HCO (29 amu) and NH_2 (16 amu) from formamide, $NHCH_3$ (30 amu) from NMF, and $N(CH_3)_2$ (44 amu) from DMF with the negative charge potentially being located on

either the N-containing or HCO fragments. In our experiment, in which the pressure of the vacuum chamber after dosing the sample was controlled at approximately 1×10^{-6} mbar, no resonant signal was observed in the ion yield curve for anions at 29 amu (HCO). Therefore, to study the DEA-induced amide bond cleavage, the ion yields for NH_2^-, $NHCH_3^-$, and $N(CH_3)_2^-$ from formamide, NMF, and DMF were measured. Resonant peaks are observed in the ion yield curves for each of these anionic fragments as shown in Figs. 2(a)–2(c).

The process of DEA in formamide proceeding through the amide bond cleavage and leading to the formation of NH_2^- can be expressed as follows:

$$HCONH_2 \xrightarrow{e} (HCONH_2)^{*-} \rightarrow HCO + NH_2^-. \quad (1)$$

First, the incoming electron attaches to a formamide molecule forming a TNI, which further decays via (C = O)-N bond dissociation. The ion yield curve of NH_2^- (16 amu) as a function of the incoming electron energy exhibits two major peaks at ~5–7 and 10 eV [Fig. 2(a)]. The 10 eV signal originates from O^- yield, which was confirmed by a previous isotopic study [33]. Thus, only the broad feature at 5–7 eV is due to NH_2^-. The feature consists of a major peak at 6.9 eV and a broad shoulder on the lower energy side centered at 5.9 eV. The position of the main peak is consistent with 6.8 eV reported by Hamann *et al.* [33] Thus, the experimental signal suggests population of at least two different TNI states responsible for efficient resonant electron capture in the energy range of 5–8 eV.

The double peak structure is even more pronounced in the case of the $NHCH_3^-$ (30 amu) signal for NMF [Fig. 2(b)]. The two peaks are centered at 5.5 and 6.7 eV and have a similar intensity. The reaction pathway for formation of $NHCH_3^-$ from NMF can be written as

$$HCONH(CH_3) \xrightarrow{e} HCONH(CH_3)^{*-} \rightarrow HCO + NHCH_3^-. \quad (2)$$

In the case of DMF, amide bond cleavage results in the formation of the anion, $N(CH_3)_2^-$, as shown in reaction scheme (3). The ion yield curve of $N(CH_3)_2^-$ (44 amu) also exhibits two distinct peaks in the region of 4.5 to 8 eV centered at 5.4 and 6.9 eV.

$$HCON(CH_3)_2 \xrightarrow{e} [HCON(CH_3)_2]^{*-} \rightarrow HCO + N(CH_3)_2^- \quad (3).$$

Importantly, a double peak structure is observed for all three ion yield curves resulting from DEA-induced amide bond cleavage. The distance between the two peaks increases with the mass of the molecules. The high energy peaks remain relatively unaffected by nitrogen atom methylation, whereas the lower energy feature shifts to lower energies.

To explain the observed resonant electron capture by formamide molecules and the double peak structure, we performed a series of electronic structure calculations aimed at characterization of the metastable electronic states that can be formed in the 5–8 eV energy range. The results of the calculations are summarized in Figs. 2–4 (See Sec. S2 for more details [27]). Both of the peaks for all three molecules lie significantly above the thermodynamic thresholds for formation of the anionic fragments (Fig. 2). To assign the double peak structure to specific metastable electronic states, we considered four possible channels of electron capture: formation of a valence shape, valence core excited, dipole-supported core-excited resonances, and doubly-excited Rydberg shake-up resonances. The calculated positions (widths) of the π^* shape resonance are 2.9 (0.42), 3.2 (0.12), and 3.4 (0.30) eV for formamide, NMF, and DMF, respectively (Table S4 [27]). This resonance, therefore, is significantly below the thermodynamic thresholds for the peptide bond cleavage. Note that all three molecules have only one valence π^* orbital. The σ^* valence resonances, if they exist, are expected to be significantly higher in energy (Sec. S2D of the Supplemental Material [27], Fig. S1). Thus, valence shape resonances can be discarded as the channels explaining DEA processes leading to amide bond cleavage. The second group of metastable states that can be populated upon electron attachment to the formamides are valence core-excited or shake-up resonances in which two valence virtual orbitals are populated and one of the originally doubly occupied orbitals is singly occupied (Fig. 1). No such state has been observed in the 5–8 eV energy range (Table S5 [27]). The third group of states are Feshbach resonances in which one of the populated virtual orbitals is the orbital corresponding to a DBS. These states can be described as states of the system with an electron trapped into a DBS of the excited neutral core. Quantitative characterization of these states, their energies and widths, is extremely challenging because of their diffuse character, doubly-excited nature (excited and electron-attached) with respect to the closed shell reference, and the high number of discretized continuum states lying below these resonances in energy. Yet, an estimate of the energies of these states can be obtained by evaluating excitation energies of the neutral molecules and the dipole moment of the resulting excited states. In the case of a large dipole moment (>2.5 D or 1.0 a.u.) [39,60,61], the resulting excited state can bind an electron forming a dipole bound state. The binding energies of electrons in the DBS are usually in the meV range; therefore, bare excitation energies of the neutral should be reliable estimates of the energies of the DBS themselves. Computed equation-of-motion coupled cluster with single and double substitution (EOM-EE-CCSD) [43,62,63] excitation energies of the singlet excited states of formamide and corresponding values of the excited states dipole moment are shown in Fig. 3. As shown, there are several

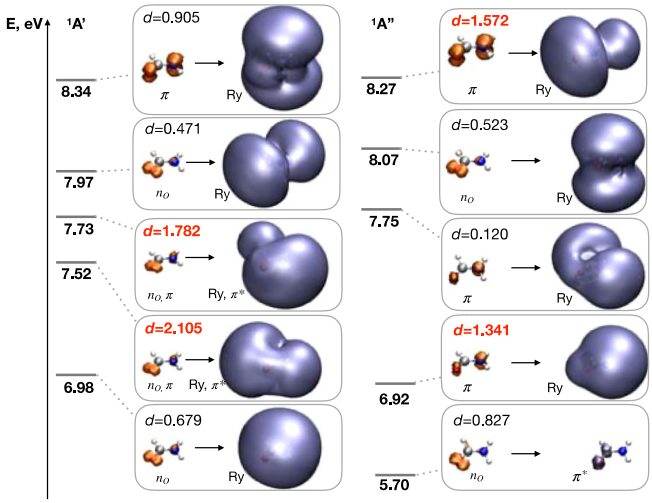

FIG. 3. EOM-EE-CCSD excitation energies (eV) for five lowest singlet A' and A'' states in formamide. Detachment and attachment densities, and the computed values of dipole moment (a.u.) are also shown [see Sec. S2F of the Supplemental Material for details [27]].

excited states of the neutral formamide in the energy range of 5–8 eV. However, all the states with a large enough dipole moment to form a DBS are located above 6.9 eV and cannot explain the low energy shoulder observed in the experimental results. The singlet-singlet excitation energies and dipole moments for NMF and DMF are listed in the Supplemental Material (Tables S7 and S8) [27].

Meanwhile, in addition to the DBSs that correlate with the singlet excited neutral core, the states that are associated with the triplet excited states of the neutral can also be populated upon electron scattering because both types of states belong to the same manifold of doublet states (Fig. 4). Indeed, "spin-forbidden" transitions are common upon electron impact and have been routinely used to study the spectroscopy of the corresponding excited states [64–67]. Ground state singlet-triplet energy gaps computed with spin-flip EOM-CCSD (EOM-SF-CCSD) [43,68,69] for neutral formamide are shown in Fig. 5. In contrast to the manifold of the singlet excited states, there is a low-energy

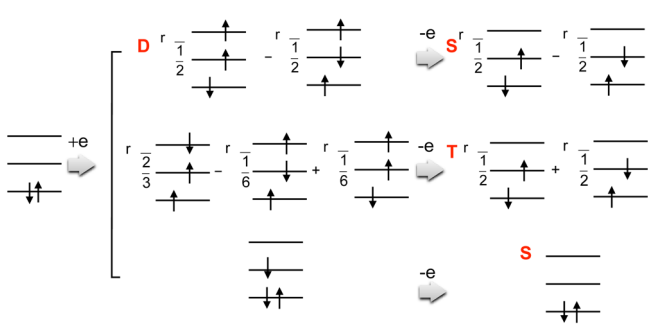

FIG. 4. Schematic electronic configurations of the electron-attached doublet states that correlate with the singlet and triplet excited states of the neutral core.

triplet $\pi\pi^*$ excited state with a large dipole moment that can capture an electron and form a DBS. The computed singlet-triplet energy gaps for NMF and DMF can be found in the Supplemental Material (Tables S7–S8). Excitation energies for the singlet and triplet excited states with a dipole moment greater than 1.0 a.u. for all three molecules are shown in Fig. 2. Importantly, the positions of both high energy and low energy peaks as well as the peak shifts between different homologues can be explained by the formation of dipole-supported resonances by both the triplet and singlet excited states of the neutral. In particular, the shift of the lower energy feature from formamide to NMF and DMF can be explained by the redshift in the excitation energy of the triplet $\pi\pi^*$ of the neutral from 5.8 to 5.6 and 5.4 eV, respectively. While the interpretation of the DEA ion yield curves presented here is solely based on the computed excitation energies and singlet-triplet energy gaps, the accuracy of the calculation is high enough (the error bars are expected to be within 0.1–0.2 eV, see Sec. S2.F1 of the Supplemental Material for more details [27]) for a reliable band assignment. Finally, a fourth group of states that could conceivably contribute to electron capture below 10 eV is associated with shake-up resonances with two electrons occupying Rydberg orbitals. These Feshbach resonances are common gateway states for electron capture in electron transmission spectroscopy and dissociative electron attachment processes [50,51]. While direct evaluation of energies and lifetimes of these resonances for large many-electron molecular systems is extremely challenging owing to very diffuse character of corresponding Rydberg orbitals in addition to their Feshbach nature, the estimates of their positions can be obtained from empirical relations to ionization potential or energy of the corresponding excited

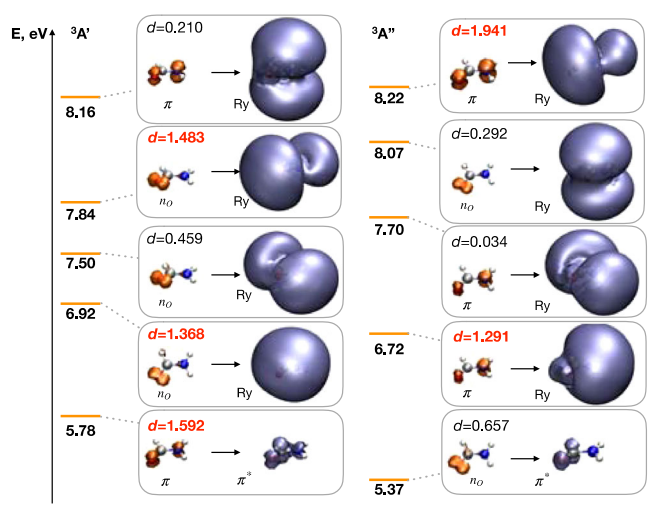

FIG. 5. EOM-SF-CCSD excitation energies (eV) for five lowest triplet A' and A'' states in formamide. Detachment and attachment densities, and the computed values of dipole moment (a.u.) are also shown (see Sec. S2 F of the Supplemental Material for details [27]).

Rydberg state of the neutral [51–56]. The linear relation between resonance energy and ionization potential [56] places the lowest $(s)^2$ Rydberg Feshbach resonance in formamide at 6.5 eV (see Sec. S2. G of the Supplemental Material [27]). Similarly, the estimates of the s^2 resonance obtained from excitation energies of the neutral are in 6.2–6.5 eV energy range. Therefore, while these resonances can contribute to the higher energy peak at 6.5–7 eV, the doubly excited Rydberg Feshbach resonance cannot explain the lower energy feature below 6 eV. Thus, in contrast to the LEE damage in DNA bases in which shape resonances play a crucial role in the low-energy range, amide bond cleavage in formamides proceeds via formation of Feshbach resonances including dipole-supported core-excited resonances, which correlate with both the singlet and triplet excited states of the neutral molecules.

To summarize, here we present combined experimental and computational investigations into the mechanism of DEA in a series of gas-phase model peptides, formamide, NMF, and DMF. We have shown that amide bond cleavage is the common dissociation mechanism for all three species. Furthermore, based on our computational studies, the DEA below 6 eV proceeds via formation of dipole-support core-excited resonances that correlate with both singlet and triplet excited states of the neutral. Whereas a detailed characterization of energetics and lifetimes of these resonances is the subject of future work, it is clear that the formation of dipole-supported resonances can be a common mechanism for the DEA to peptides, and this requires further exploration via both theory and experiments.

This material is based upon work supported by the U.S. Department of Energy Office of Science, Office of Basic Energy Sciences under Award No. DE-FC02-04ER15533 (to Z. L., M. R., M. M. D., I. C., and S. P.), and National Science Foundation (CHE-1665276 to K. B. B.). This is contribution number NDRL 5211 from the Notre Dame Radiation Laboratory.

*These authors contributed equally to this work.
†Corresponding author.
bravaya@bu.edu
‡Corresponding author.
sptasins@nd.edu

[1] E. Alizadeh, T. M. Orlando, and L. Sanche, Biomolecular damage induced by ionizing radiation: The direct and indirect effects of low-energy electrons on DNA, Annu. Rev. Phys. Chem. **66**, 379 (2015).
[2] L. Sanche, Nanoscopic aspects of radiobiological damage: Fragmentation induced by secondary low-energy electrons, Mass Spectrom. Rev. **21**, 349 (2002).
[3] B. Boudaïffa, P. Cloutier, D. Hunting, M. A. Huels, and L. Sanche, Resonant formation of DNA strand breaks by low-energy (3 to 20 eV) electrons, Science **287**, 1658 (2000).
[4] I. Baccarelli, I. Bald, F. A. Gianturco, E. Illenberger, and J. Kopyra, Electron-induced damage of DNA and its components: Experiments and theoretical models, Phys. Rep. **508**, 1 (2011).
[5] J. Gu, J. Leszczynski, and H. F. Schaefer, Interactions of electrons with bare and hydrated biomolecules: From nucleic acid bases to DNA segments, Chem. Rev. **112**, 5603 (2012).
[6] L. Sanche, Low energy electron-driven damage in biomolecules, Eur. Phys. J. D **35**, 367 (2005).
[7] E. Alizadeh and L. Sanche, Precursors of solvated electrons in radiobiological physics and chemistry, Chem. Rev. **112**, 5578 (2012).
[8] J. D. Gorfinkiel and S. Ptasińska, Electron scattering from molecules and molecular aggregates of biological relevance, J. Phys. B **50**, 182001 (2017).
[9] R. Panajotovic, F. Martin, P. Cloutier, D. Hunting, and L. Sanche, Effective cross sections for production of single-strand breaks in plasmid DNA by 0.1 to 4.7 eV electrons, Radiat. Res. **165**, 452 (2006).
[10] J. Simons, How do low-energy (0.1–2 eV) electrons cause DNA-strand breaks?, Acc. Chem. Res. **39**, 772 (2006).
[11] R. Barrios, P. Skurski, and J. Simons, Mechanism for damage to DNA by low-energy electrons, J. Phys. Chem. B **106**, 7991 (2002).
[12] H. Abdoul-Carime, P. Cloutier, and L. Sanche, Low-energy (5–40 eV) electron-stimulated desorption of anions from physisorbed DNA bases, Radiat. Res. **155**, 625 (2001).
[13] R. J. Boohaker, M. W. Lee, P. Vishnubhotla, J. M. Perez, and A. R. Khaled, The use of therapeutic peptides to target and to kill cancer cells, Curr. Med. Chem. **19**, 3794 (2012).
[14] K. Fosgerau and T. Hoffmann, Peptide therapeutics: Current status and future directions, Drug Discov. Today **20**, 122 (2015).
[15] S. M. Pimblott and J. A. LaVerne, Production of low-energy electrons by ionizing radiation, Radiat. Phys. Chem. **76**, 1244 (2007).
[16] J. Berdys, P. Skurski, and J. Simons, Damage to model DNA fragments by 0.25–1.0 eV electrons attached to a thymine π^* orbital, J. Phys. Chem. B **108**, 5800 (2004).
[17] J. Berdys, I. Anusiewicz, P. Skurski, and J. Simons, Damage to model DNA fragments from very low-energy (<1 eV) electrons, J. Am. Chem. Soc. **126**, 6441 (2004).
[18] J. Berdys, I. Anusiewicz, P. Skurski, and J. Simons, Theoretical study of damage to DNA by 0.2–1.5 eV electrons attached to cytosine, J. Phys. Chem. A **108**, 2999 (2004).
[19] R. A. Zubarev, N. L. Kelleher, and F. W. McLafferty, Electron capture dissociation of multiply charged protein cations. A nonergodic process, J. Am. Chem. Soc. **120**, 3265 (1998).
[20] J. Simons, Mechanisms for S—S and N—C_α bond cleavage in peptide ECD and ETD mass spectrometry, Chem. Phys. Lett. **484**, 81 (2010).
[21] F. Tureček and R. R. Julian, Peptide radicals and cation radicals in the gas phase, Chem. Rev. **113**, 6691 (2013).
[22] M. Stepanovic, Y. Pariat, and M. Allan, Dissociative electron attachment in cyclopentanone, γ-butyrolactone, ethylene carbonate, and ethylene carbonate-d4: Role of dipole-bound resonances, J. Chem. Phys. **110**, 11376 (1999).
[23] A. M. Scheer, K. Aflatooni, G. A. Gallup, and P. D. Burrow, Bond breaking and temporary anion states in uracil and

halouracils: Implications for the DNA bases, Phys. Rev. Lett. **92**, 068102 (2004).

[24] T. Sommerfeld, H.-D. Meyer, and L. S. Cederbaum, Potential energy surface of the CO_2^- anion, Phys. Chem. Chem. Phys. **6**, 42 (2004).

[25] T. Sommerfeld, Dipole-bound states as doorways in (dissociative) electron attachment, *J. Phys. Conf. Ser.* 4, 245 (2005).10.1088/1742-6596/4/1/036

[26] T. Sommerfeld, Intramolecular electron transfer from dipole-bound to valence orbitals: Uracil and 5-chlorouracil, J. Phys. Chem. A **108**, 9150 (2004).

[27] See Supplemental Material http://link.aps.org/supplemental/10.1103/PhysRevLett.122.073002 for the experimental setup and computational details, which includes Refs. [28–57].

[28] P. Cicman, G. Senn, G. Denifl, D. Muigg, J. D. Skalny, P. Lukac, A. Stamatovic, and T. M. Märk, Dissociative electron attachment to CO_2, Czech. J. Phys. **48**, 1135 (1998).

[29] M. Feyereisen, G. Fitzgerald, and A. Komornicki, Use of approximate integrals in *ab initio* theory. An application in MP2 energy calculations, Chem. Phys. Lett. **208**, 359 (1993).

[30] F. Weigend, Häser, RI-MP_2: First derivatives and global consistency, Theor. Chem. Acc. **97**, 331 (1997).

[31] R. A. Distasio, Jr., R. P. Steele, Y. M. Rhee, Y. Shao, and M. Head-Gordon, An improved algorithm for analytical gradient evaluation in resolution-of-the-identity second-order Møller-Plesset perturbation theory: Application to alanine tetrapeptide conformational analysis, J. Comput. Chem. **28**, 839 (2007).

[32] C. Desfrançois, V. Périquet, S. Carles, and J. P. Schermann, Experimental and *ab initio* theoretical studies of electron binding to formamide, N-methylformamide, and N,N-dimethylforamide, J. Chem. Phys. **110**, 4309 (1999).

[33] T. Hamann, A. Edtbauer, F. F. da Silva, S. Denifl, P. Scheier, and P. Swiderek, Dissociative electron attachment to gas-phase formamide, Phys. Chem. Chem. Phys. **13**, 12305 (2011).

[34] G. D. Purvis, III and R. J. Bartlett, A full coupled-cluster singles and doubles model: The inclusion of disconnected triples, J. Chem. Phys. **76**, 1910 (1982).

[35] R. J. Kurland and E. B. Wilson, Jr., Microwave spectrum, structure, dipole moment, and quadrupole coupling constants of formamide, J. Chem. Phys. **27**, 585 (1957).

[36] A. C. Fantoni and W. Caminati, Rotational Spectrum and *ab initio* Calculations of N-methylformamide, J. Chem. Soc., Faraday Trans. **92**, 343 (1996).

[37] R. M. Meighan and R. H. Cole, Dielectric properties of alkyl amides. I. Vapor phase dipole moments and polarization in benzene solution[1], J. Phys. Chem. **68**, 503 (1964).

[38] J. M. Herbert, *The Quantum Chemistry of Loosely-Bound Electrons* (John Wiley & Sons, Inc, 2015), pp. 391–517.

[39] K. D. Jordan and F. Wang, Theory of dipole-bound, Annu. Rev. Phys. Chem. **54**, 367 (2003).

[40] T.-T. Chen, J. Simons, and K. D. Jordan, Analysis of the equation-of-motion theory of electron affinities and ionization potentials, Chem. Phys. **14**, 145 (1976).

[41] J. Simons and W. D. Smith, Theory of electron affinities of small molecules, J. Chem. Phys. **58**, 4899 (1973).

[42] M. Nooijen and R. J. Bartlett, Equation of motion coupled cluster method for electron attachment, J. Chem. Phys. **102**, 3629 (1995).

[43] A. I. Krylov, Equation-of-motion coupled-cluster methods for open-shell and electronically excited species: The Hitchhiker's guide to Fock space, Annu. Rev. Phys. Chem. **59**, 433 (2008).

[44] T.-C. Jagau, D. Zuev, K. B. Bravaya, E. Epifanovsky, and A. I. Krylov, A fresh look at resonances and complex absorbing potentials: Density matrix based approach, J. Phys. Chem. Lett. **5**, 310 (2014).

[45] D. Zuev, T.-C. Jagau, K. B. Bravaya, E. Epifanovsky, Y. Shao, E. Sundstrom, M. Head-Gordon, and A. I. Krylov, Complex absorbing potentials within EOM-CC family of methods: Theory, implementation, and benchmarks, J. Chem. Phys. **141**, 024102 (2014).

[46] A. Ghosh, N. Vaval, S. Pal, and R. J. Bartlett, Complex absorbing potential based equation-of-motion coupled cluster method for the potential energy curve of CO_2^- anion, J. Chem. Phys. **141**, 164113 (2014).

[47] T.-C. Jagau, K. B. Bravaya, and A. I. Krylov, Extending quantum chemistry of bound states to electronic resonances, Annu. Rev. Phys. Chem. **68**, 525 (2017).

[48] A. A. Kunitsa, A. A. Granovsky, and K. B. Bravaya, CAP-XMCQDPT2 method for metastable electronic states, J. Chem. Phys. **146**, 184107 (2017).

[49] H. H. Falden, K. R. Falster-Hansen, K. L. Bak, S. Rettrup, and S. P. Sauer, Benchmarking second order methods for the calculation of vertical electronic excitation energies: Valence and Rydberg states in polycyclic aromatic hydrocarbons, J. Phys. Chem. A **113**, 11995 (2009).

[50] G. J. Schulz, Resonances in electron impact on diatomic molecules, Rev. Mod. Phys. **45**, 423 (1973).

[51] B. C. Ibănescu, O. May, A. Monney, and M. Allan, Electron-induced chemistry of alcohols, Phys. Chem. Chem. Phys. **9**, 3163 (2007).

[52] L. Sanche and G. J. Schulz, Electron transmission spectroscopy: Resonances in triatomic molecules and hydrocarbons, J. Chem. Phys. **58**, 479 (1973).

[53] L. Sanche and G. J. Schulz, Vibrational progressions and Rydberg series of O_2^- and NO^-, Phys. Rev. Lett. **27**, 1333 (1971).

[54] L. Sanche and G. J. Schulz, Electron transmission spectroscopy: Rare gases, Phys. Rev. A **5**, 1672 (1972).

[55] L. Sanche and G. J. Schulz, Electron transmission spectroscopy: Core-excited resonances in diatomic molecules, Phys. Rev. A **6**, 69 (1972).

[56] D. Spence, Prediction of low energy molecular Rydberg states from Feshbach resonance spectra, J. Chem. Phys. **66**, 669 (1977).

[57] M. M. Dawley and S. Ptasińska, Dissociative electron attachment to gas-phase N-methylformamide, Int. J. Mass Spectrom. **365–366**, 143 (2014).

[58] G. Hart-Smith, A review of electron-capture and electron-transfer dissociation tandem mass spectrometry in polymer chemistry, Anal. Chim. Acta **808**, 44 (2014).

[59] Z. Li, A. R. Milosavljević, I. Carmichael, and S. Ptasinska, Characterization of neutral radicals from a dissociative electron attachment process, Phys. Rev. Lett. **119**, 053402 (2017).

[60] C. Desfrançois, H. Abdoul-Carime, N. Khelifa, J. P. Schermann, V. Brenner, and P. Millie, Dipole binding: An experimental test for small cluster structure calculations, J. Chem. Phys. **102**, 4952 (1995).

[61] C. Desfrançois, H. Abdoul-Carime, and J.-P. Schermann, Ground-state dipole-bound, Int. J. Mod. Phys. B **10**, 1339 (1996).

[62] J. F. Stanton and R. J. Bartlett, The equation of motion coupled-cluster method. A systematic biorthogonal approach to molecular excitation energies, transition probabilities, and excited state properties, J. Chem. Phys. **98**, 7029 (1993).

[63] J. Geertsen, M. Rittby, and R. J. Bartlett, The equation-of-motion coupled-cluster method: Excitation energies of Be and CO, Chem. Phys. Lett. **164**, 57 (1989).

[64] A. Kuppermann, W. M. Flicker, and O. A. Mosher, Electronic spectroscopy of polyatomic molecules by low-energy, variable-angle electron Impact, Chem. Rev. **79**, 77 (1979).

[65] J. P. Doering, Jr. and J. H. Moore, Observation of a singlet—Triplet transition in gas phase pyridine by ion and electron impact, J. Chem. Phys. **56**, 2176 (1972).

[66] K. Regeta, M. Allan, Z. Mašín, and J. D. Gorfinkiel, Absolute cross sections for electronic excitation of Pyrimidine by electron impact, J. Chem. Phys. **144**, 024302 (2016).

[67] E. H. Van Veen, Triplet $\pi \rightarrow \pi^*$ Transitions in thiophene, furan and pyrrole by low-energy electron-impact spectroscopy, Chem. Phys. Lett. **41**, 535 (1976).

[68] A. I. Krylov, Size-consistent wave functions for bond-breaking: The equation-of-motion spin-flip model, Chem. Phys. Lett. **338**, 375 (2001).

[69] A. I. Krylov, Spin-flip equation-of-motion coupled-cluster electronic structure method for a description of excited states, bond breaking, diradicals, and triradicals, Acc. Chem. Res. **39**, 83 (2006).